EPiC Series in Built Environment

Volume 4, 2023, Pages 659–667

Proceedings of 59th Annual Associated Schools of Construction International Conference

Spatial Discrepancies between Close-Range Photogrammetry and Terrestrial-LiDAR Models

Gustavo Maldonado, Ph.D., PE, Abdoul Ouangre, M.S., William Stevick, M.S., Marcel Maghiar, Ph.D., CM-BIM, Soonkie Nam, Ph.D.
Georgia Southern University
Statesboro, Georgia, USA

This article investigates spatial discrepancies existing between two simple, close-range photogrammetry (CRP) models and a terrestrial light detection and ranging (T-LiDAR) model. The latter is more accurate and serves as benchmark. The commonly modeled zone is a six-acre commercial property. All three models were georeferenced in the same coordinate system before acquiring spatial coordinates of 50 common points from each of them. Two models were produced via CRP, employing Agisoft's Metashape Professional software, and one, the benchmark model, was generated using Leica Geosystems' C10 scanner. This laser-based model used Leica's Visual Alignment procedure for registration purposes. This approach is not the most accurate available today, however, it requires minimal target acquisitions and saves considerable time in the field. One of the CRP models was built with pictures taken from an UAV flying at an approximate 76-ft altitude over ground level. The second CRP model was produced with pictures taken from a 116-ft altitude. Fifty positions and 1,225 distance discrepancies were calculated for each CRP model with respect to the same points and distances acquired from the T-LiDAR model. The compared distances ranged from 0.02 to 415.50 ft. A statistical analysis of those discrepancies is presented in this paper.

Key Words: Close-Range Photogrammetry, LiDAR, Distance Discrepancy

Introduction

Nowadays, CRP via Unmanned Aerial Vehicles (UAVs or 'drones') is often employed in the Architectural, Engineering and Construction (AEC) industry for a variety of useful purposes. This low-cost alternative to 3D laser scanning is becoming commonly used in construction related projects, including virtual surveying, capture of as-built conditions for predesign/design activities, monitoring of construction progress, determination of pay quantities, etc. More than a decade ago, Remondino et al. (2011) already presented an overview of existing UAV systems, especially those employed in geomatics applications. They described the status and future perspectives of UAV photogrammetry for mapping and 3D modeling. More recently, Li and Liu (2019) indicated numerous current applications of the use

of drones in the construction industry, especially in land surveying, logistics, on-site construction, maintenance and demolition. Luhmann (2019) described recent developments in CRP indicating that "In industrial applications, the verification of the achieved accuracy with respect to accepted guidelines is most important. In most cases, standardized characteristics such as the maximum length measurement error have to be reported…" Even though CRP is now ubiquitous, not all users know the technical and scientific aspects of this technique or even the actual spatial accuracies that could be attained in their resulting 3D models. There are numerous factors contributing to those accuracies. Two significant ones are the quality/resolution of the employed cameras and the altitude from where pictures are taken. They are critical in determining the size of a detail that could be distinguished in a single pixel. The estimation of the attained spatial accuracies in the final CRP models, when using currently affordable drones, has motivated the completion of the work reported here.

The objective of this study is to determine statistical discrepancies in distances extracted from three different models of the same existing spatial conditions. Two of these virtual models are CRP ones and their extracted distances were compared against a more accurate T-LiDAR model, which served as benchmark. The generation of the resulting CRP models require minimum knowledge of CRP techniques, as the user only needs to know how to fly an UAV and how to employ a commercially available CRP software package.

The selected modeled area is a 6-acre commercial property, Fusion Gymnasium, in Statesboro, GA. One of the CRP models was built with pictures taken at an average altitude of 76-ft over the ground and is herein referred to as the 76'-CRP model. The other CRP model was produced with pictures taken from a 116-ft altitude and is herein referred to as the 116'-CRP model. Since both CRP models used the same camera and resolution, it was expected that the low-altitude one will be able to distinguish more details and, consequently, be more accurate than the high-altitude model.

The selected T-LiDAR benchmark model employed 47 scans and was generated via a registration procedure known as Leica's Visual Alignment. This approach is less accurate than a target-based registration, but it requires minimum target acquisition in the field and allows for a faster completion of the required field scans. Nevertheless, Visual Alignment requires more human intervention and data processing time in a computer laboratory than a target-based registration process. Several recent studies have completed distance-discrepancy analyses involving T-LiDAR models. They include the work by Maldonado et al. (2020) where the discrepancy between georeferenced and non-georeferenced models were investigated. A year ago, Maldonado et al. (2021) estimated the error introduced by georeferencing a point-cloud model via an accurate closed-traverse survey. Additionally, recently, Maldonado et al. (2022) analyzed distance discrepancies in T-LiDAR models georeferenced via Static GNSS vs Rapid RTK GNSS.

Instruments and Methodology

This work employed four main instruments. They are shown in Figure 1 and their characteristics are briefly described in this paragraph: (1) A 1-sec robotic, total-station device from Leica Geosystems, TRCP 1201+ R1000. Its manufacturer indicates (Leica 2021) this instrument has a range of 1,500 m (~1,640 yd) when used with a 360° reflector prism, under light haze with visibility of 20 km (~21,900 yd). In reflector mode, the standard deviation σ of its error, for a single-distance measurement, is σ = 1 mm+1.5 ppm×(distance < 3000 m). In US Customary units, that accuracy is equivalent to σ = 0.04 in+1.5 ppm×(distance < 3,281 yd). Its angular accuracies are 1 arcsecond for horizontal and vertical angles. This total-station instrument was used with a 360° reflector prism, Leica's GRZ4, to complete

a closed-traverse procedure. This resulted in the establishments of six fixed, ground, control points within the area to be modeled. (2) A laser-based scanner, Leica Geosystems' ScanStation C10, was employed to generate a 3D point-cloud model of the selected area and structure for comparison purposes. According to Leica Geosystems (Leica 2022), this scanner has a position accuracy of 6 mm (0.24 in) and measurement accuracy of 4 mm (0.16 in), both are 1σ at 1-50 m range (1.1-54.7 yd range). This scanner has a dual-axis compensator with horizontal and vertical angular accuracies of 12 seconds. Its scanning range is 300 m (328 yd) at 90% albedo and 134 m (146.5 yd) at 18% albedo. Its maximum scanning rate is 50,000 points per second. (3) An UAV from Da-Jiang Innovations (DJI) was used to capture the pictures leading to the generation of two 3D, close-range, photogrammetric models. This small commercially available drone is the DJI Mavic 2 Pro. It weighs 907 grams and carries a 20-megapixel camera, mounted on a three-axis gimbal for stabilization purposes. Additional specifications can be found at DJI's website (DJI, 2022). (4) A Topcon AT-B2 Automatic Level instrument was employed to obtain differential elevations among the six fixed, ground points used to georeference the resulting three virtual models of this project. Topcon Corporation (Topcon, 2022) indicates that this device has a 32x-magnification eyepiece and a dampened compensator able to level the line of sight within a range of ±15 arcminutes, with a setting accuracy of 0.3 arcsecond. Additionally, Topcon specifies that this device, when used with a leveling rod without micrometer, can complete a 1-km, double-run, leveling procedure with an accuracy of 0.7 mm (0.03 in).

(a) (b) (c) (d) (e)

Figure 1. Employed devices: (a) DJI's Mavic 2 Pro; (b) Leica's Robotic Total Station TCRP 1201+ R1000, (c) & (d) Leica's ScanStation C10, (e) Topcon's AT-B2 Auto Level

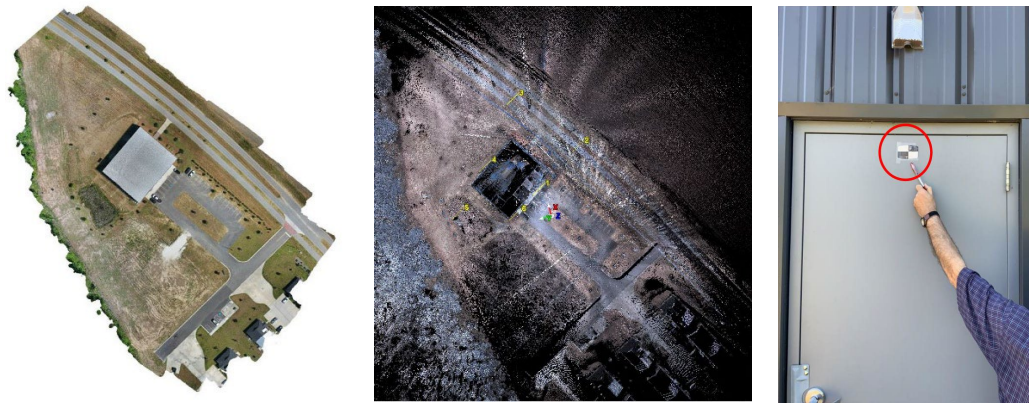

(a) (b) (c)

Figure 2. Plan Views: (a) Photo-based model from 116 ft; (b) 3D, T-LiDAR Model (North is approximately upward in both pictures); (c) Example of sticker to identify a secondary point.

In this study, the modeled commercial property encompassed 6 acres. It included a gymnasium building, its parking lot, and surrounding grassy zones (see Figure 2). Three models were generated to compare their relative accuracies: 76'-CRP, 116'-CRP, and T-LiDAR models. The employed methodology involved ten different tasks:

(I) Initially, six ground control points were established within the site. Their spatial coordinates where accurately determined, within a selected local system of reference, via a closed-traverse procedure. This approach resulted in an initial horizontal error of closure of 0.023 ft and in a longitudinal precision of 1 in 31,397. The local system of reference was selected by assigning the following coordinates to vertex 1: Easting = 400.000 ft, Northing = 800.000 ft, Elevation = 100.000, and by selecting an arbitrary value, 60°, for azimuth 1→2. Table 1 shows the final balanced coordinates of all 6 ground control points. Later, these coordinates were employed to georeference, into the same common system, the resulting three virtual models.

Table 1

Balanced Local Coordinates of Ground Control Points via Closed Traverse

Vertex	EASTING X (ft)	NORTHING Y (ft)	ELEVATION Z (ft)
1	400.000	800.000	100.000
2	500.800	858.196	102.457
3	405.187	987.789	100.936
4	312.529	877.556	99.561
5	230.620	803.535	96.391
6	339.238	766.424	99.156

Tasks **(II)-(V)** are related to the generation of the two CRP models: **(II)** Before scanning or taking pictures, more than 100 highly visible, black-&-white stickers (~ 10 cm × 6.5 cm each) where placed on walls, doors, window frames, light posts, sidewalks, pavements, mailbox, and other objects contained within the area to be modeled. See sample sticker on Figure 2c. These points are herein referred to as Secondary Points. Their locations were to be identified later, within each of the three models, to extract their coordinates and distances between them. **(III)** In this task, the Mavic 2 Pro UAV was flown over the site by our Lab Manager, Mr. Shawn Jackson, who is a licensed Remote Pilot by the Federal Aviation Administration. The drone was programmed to automatically take necessary overlapping pictures. Two different sets of pictures were acquired, one from an average 76' altitude, over the ground, and the other from an averaged 116' altitude. These altitudes were reported during data processing by the employed CRP software package. Task **(IV)** consisted in using Agisoft's Metashape Pro software (version 1.7.1 built 11797), in the BEaM laboratory, to generate the 76'-CRP and the 116'-CRP virtual models, one from each set of pictures. During task **(V)**, the resulting two 3D photo-based models were georeferenced into the same selected local coordinate system. For this purpose, within each virtual model, markers were placed on identified locations of the corresponding control points listed in Table 1. Then, the coordinates of these control points were imported into the CRP models to define scaling bars within each of them. The lengths of these bars were pythagorically calculated from the coordinates in Table 1. A few of the characteristic parameters for the resulting 76'-CRP and 116'-CRP models, including RMSE values, are presented in Tables 2 and 3, respectively.

Tasks **(VI)-(VIII)** are associated with the generation of the T-LiDAR model: Task **(VI)** consisted in laser scanning the site with Leica's ScanStation C10. A total of forty-five (45) exterior and two (2) interior scans were completed to cover the selected area. This took approximately 35-45 minutes per scan. In Task **(VII)**, unwanted noise (i.e., solar beams, and vehicular/pedestrian traffic) was removed from each scan. During this task, the Leica's Visual Alignment registration (stitching) procedure was employed to build an initial, non-georeferenced point-cloud model. This scheme consisted of stitching two neighboring scans at a time to grow and build a fully stitched point-cloud, the T-LiDAR model. This approach saved considerable scanning time in the field but increased the post-processing time in the laboratory. This manual stitching procedure is less accurate than a target-based registration which requires more time in the field. The 6 ground control points were scanned by using white, spherical, six-inch-diameter targets, placed on poles of known heights, over their respective ground nails. All scans were completed at medium resolution which corresponds to a separation of 10 cm (~3.94 in) between scanned points when they are at 100 m (~328.1 ft) from the scanner. During task **(VIII)** the full T-LiDAR model was georeference in the same local coordinate system used by the CRP models. This required to import the coordinates of the 6 ground control points from a text file which served as an additional small scan file (containing only those 6 points). Then, their locations were matched via a least-square scheme with those of the same points already scanned and included in the point cloud.

Table 2

Characteristics of the Two Photo-Based Models (According to the Metashape Software)

Flying Altitude (ft)	Number of Images	Aligned Cameras	Covered Area yd^2	Ground Resolution ft/pix	Control Points	Check Points	Scale Bars
76	600	589	27,600	0.0165	6	50	6
116	464	461	33,300	0.0253	6	50	6

Table 3

Root Mean Square Errors Reported by Metashape for 6 Control Markers and 50 Check Points

	X (ft)	Y (ft)	Z (ft)	XY (ft)	Total (ft)
CRP Model	(6) Control Markers				
75-ft	0.242	0.168	0.266	0.294	0.397
116-ft	0.234	0.156	0.192	0.341	0.384
CRP Model	(50) Check Points				
75-ft	0.107	0.101	0.219	0.148	0.264
116-ft	0.227	0.214	0.226	0.385	0.915

Tasks **(IX)** and **(X)** lead to the statistics of discrepancies in lengths extracted from the finalized 3 models: Task **(IX)** involved all 3 georeferenced virtual models, 76'-CRP, 116'-CRP, and T-LiDAR. It consisted in identifying 50 auxiliary points, common to all 3 models. The spatial coordinates of these points were extracted 3 times, one from each model. Even though these 50 points were the same in all 3 final virtual models, their coordinates showed small discrepancies from one model to another. During

task **(X)**, the distances between each auxiliary point and the remaining 49 auxiliary points were pythagorically determined within the same model. This resulted in a total of 1,225 non-repeated distances from each model. This was done 3 times, one per model. Then, these distances were compared to determine the statistics of the discrepancies of each CRP model with respect to the same distances extracted from the T-LiDAR model.

Results

The above methodology led to the identification of 50 common auxiliary points in all 3 resulting virtual 3D models. For each auxiliary point, 3 sets of coordinates were acquired. One set from each of the 3 models (76'-CRP, 116'-CRP, and T-LiDAR). All discrepancies were determined with respect to the more accurate model, T-LiDAR, which served as benchmark. That is, the position discrepancies were calculated by vectorially subtracting the fifty T-LiDAR positions from the corresponding fifty 76'-CRP positions and also from the fifty 116'-CRP positions. This resulted in two position discrepancies for each of the fifty auxiliary points, one for the 76'-CRP model and one for the 116'-CRP model, both versus the T-LiDAR model. Their statistics are presented in Table 4, where it can be observed that the mean values of the discrepancies are not zero. Therefore, the standard deviation of the population (STD_P) or of the sample (STD_S) do not coincide with their respective root mean square values (RMSV).

Since the RMSV is a measure of the magnitude of a set of numbers, which in this case are position discrepancies, we focused on this parameter to compare the position discrepancies of both photo-based models with respect to the LiDAR model.

Table 4

Statistics of two types of discrepancies: (a) Position discrepancies of 50 auxiliary points. (b) Distance discrepancies among those 50 points (1225 non-repeated distances).

Statistic Function	76'-CRP Model vs T-LiDAR Model		116'-CRP Model vs T-LiDAR Model	
	Position Discrepancies (ft)	Distance Discrepancies (ft)	Position Discrepancies (ft)	Distance Discrepancies (ft)
Max =	1.955	1.798	1.997	1.769
Min =	0.000	-1.473	0.037	-1.547
Mean =	0.364	0.165	0.470	0.329
Median =	0.301	0.150	0.331	0.310
STD_P =	0.330	0.299	0.372	0.428
STD_S =	0.333	0.299	0.376	0.428
RMSV =	0.491	0.341	0.599	0.540

The RMSV of the position discrepancy for the 76'-CRP model is $RMSV_{76\text{-ft}} = 0.49$ ft, whereas for the 116'-CRP model, is $RMSV_{116\text{-ft}} = 0.60$ ft. This is consistent with the expected result. That is, the lower-altitude close-range photogrammetric model should present less error with respect to the LiDAR model than the higher-altitude one.

Figures 3 and 4 show the discrepancy in the 1,225 non-repeated distances among the fifty auxiliary points. Their lengths ranged from 0.015 ft to 415.504 ft. Figure 3 shows the distance discrepancies between the 76'-CRP and LiDAR models. Figure 4 depicts the distance discrepancies between the 116'-CRP and LiDAR models.

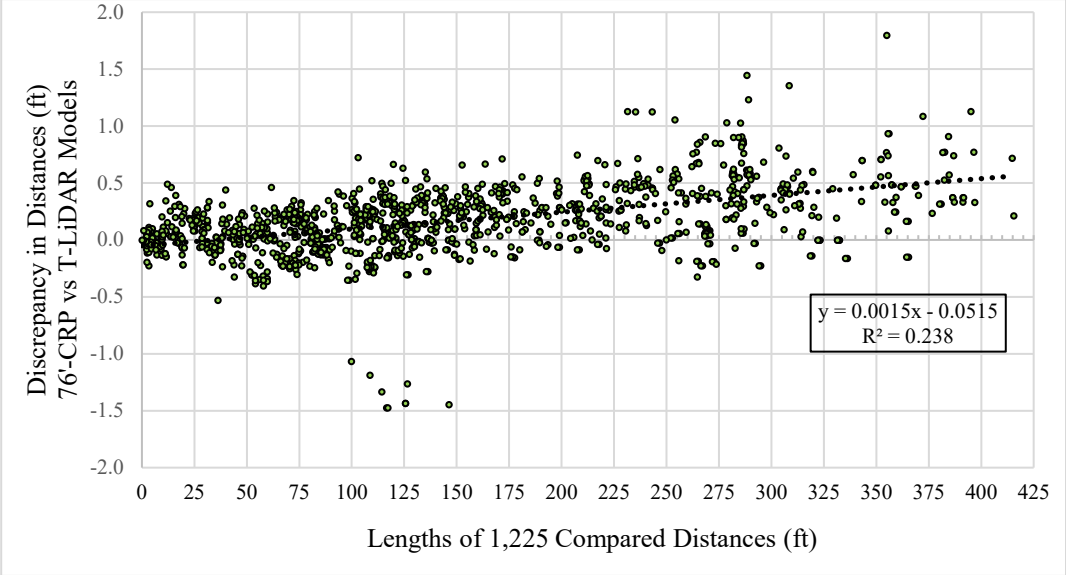

Figure 3. Discrepancies in lengths. T-LiDAR Distances Subtracted from 76'-CRP Distances

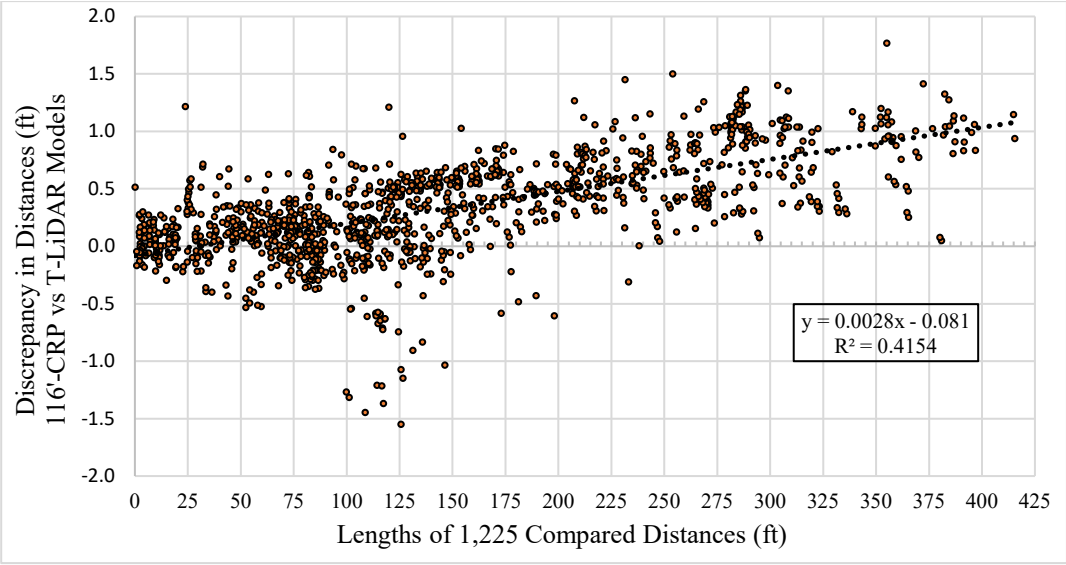

Figure 4. Discrepancies in lengths. T-LiDAR Distances Subtracted from 116'-CRP Distances

Both figures, 3 and 4, show a trend line and include the expressions of their corresponding linear regressions along with their respective coefficients of determination (R^2 values). For the 76'-CRP model, $R^2 \approx 24\%$, whereas for the 116'-CRP model $R^2 \approx 42\%$. This coefficient is an indication of the extent that the variance of distance discrepancies is explained by the variance in the magnitude of the lengths of those distances. Figure 5 shows pictures of two finalized models.

(a) (b)

Figure 5. Views of Final Models: (a) 116'-CRP Model, and (b) T-LiDAR Model

Final Remarks and Conclusions

This work consisted in generating 3 different virtual 3D models of the same existing conditions on a 6-acre commercial area and in determining their spatial discrepancies. For this, the Cartesian coordinates of the same 50 points were acquired from each of the 3 different models. Two models were produced via CRP and one, the most accurate, was generated using a T-LiDAR scanner, via a semi-manual registration procedure, Leica Geosystems' Visual Alignment. One of the CRP models was built with pictures taken from a 76-ft-average altitude flight above ground. The second CRP model was produced with pictures taken from an approximate altitude of 116 ft. Fifty positions and 1,225 non-repeated distances among them were considered to calculate the spatial discrepancies of each CRP model with respect to the same points and distances acquired from within the T-LiDAR model. The 1,225 compared distances ranged from 0.015 to 415.50 ft. Since several points and distances presented large discrepancies, their coordinates were double checked and reacquired, but remained with the same original values. Therefore, those few large discrepancy magnitudes stayed as valid data in this study.

After completion of the statistical analyses, the following remarks and conclusions are presented:

1. The largest discrepancies of the CRP models, with respect to the T-LiDAR model, are associated to points acquired in excessively deformed areas of the resulting photogrammetric models.

2. Regarding point-position measurements, the 76'-CRP model is 1.22 times more precise than the 116'-CRP model. This factor was determined by using the following ratio of RMSVs:

$$\frac{RMSV_{Position\ Discrp.\ of\ CRP\ Model_{116-ft}}}{RMSV_{Position\ Discrp.\ of\ CRP\ Model_{76-ft}}} = \frac{0.599\ ft}{0.491\ ft} = 1.22$$

3. Regarding distance measurements, the 76'-CRP model is 1.58 times more precise than the 116'-CRP model. This factor was determined by using the following ratio of RMSVs:

$$\frac{RMSV_{Distance\ Discrp.\ of\ CRP\ Model_{116-ft}}}{RMSV_{Distance\ Discrp.\ of\ CRP\ Model_{76-ft}}} = \frac{0.540\ ft}{0.341\ ft} = 1.58$$

4. In Figures 3 and 4 it is observed that the discrepancies in the distances are becoming more positive as the magnitude of the measured lengths increases. This trend is captured by the linear regressions included in those figures. That is, the distance discrepancies of the 116'-CRP model (with respect to the T-LiDAR model) tend to increase more with the magnitude of the measured lengths than the distance discrepancies of the 76'-CRP model (with respect to the T-LiDAR model).

References

DJI (2022), Mavic 2 Specs. Available at the below link, accessed on October 29, 2022: https://www.dji.com/mavic-2/info#specs

Li, Y., & Liu, C. (2019). Applications of multirotor drone technologies in construction management. International Journal of Construction Management, 19(5), 401–412.

Leica (2021), Leica TPS 1200 Series Technical Data (2022). 16 pages. Available at the below link, accessed on Oct 29, 2022: https://osdc.ca/wp-content/uploads/2015/07/TPS1200_TechnicalData.pdf

Leica (2022), Leica ScanStation C10. The All-in-One Laser Scanner for Any Application. Available at the below link, accessed on Nov 14, 2021: https://lib.store.yahoo.net/lib/yhst-141816440267150/Leica-ScanStation-C10-DataSheet.pdf

Luhmann, T. (2019). Recent Developments in Close-Range Photogrammetry. GIM International Magazine, February 14, 2019. Available at the below link, accessed on December 15, 2022: https://www.gim-international.com/content/article/recent-developments-in-close-range-photogrammetry

Topcon (2022), AT-B Series Auto Level, Available at the below link, accessed on Oct 29, 2022: https://www.topcon.co.jp/en/positioning/products/pdf/AT-B2_AT-B3A_AT-B4A_E.pdf

Maldonado, G.O., Maghiar, M., Tharp, B., and Patel, D., (2020). Point-Cloud Models of Historic Barns – Spatial Discrepancies of Laser Scanning versus Robotic Total Station. ASC 2020 56th Annual ASC International Conference, (Epic Series in Built Environment, Vol 1), pp 292-300.

Maldonado, G.O., Maghiar, M., and Augustine, A., (2021). Comparison of Distance Discrepancies in Georeferenced and Non-Georeferenced Terrestrial LiDAR Models. ASC 2021 57th Annual ASC International Conference, (Epic Series in Built Environment, Vol 2), pp 311-319.

Maldonado, G.O., Ibrahim, U., Purcell, R., Nam, S., and Maghiar, M., (2022). Distance Discrepancies in T-LiDAR, Point-Cloud Models Georeferenced via RTK and Static GNSS. ASC 2022 58th Annual ASC International Conference, (Epic Series in Built Environment, Vol 3), pp 434-442.

Remondino, F., Barazzetti, L., Nex, F., Scaioni, M., and Sarazzi, D., (2011). UAV Photogrammetry for Mapping and 3D Modeling –Current Status and Future Perspectives–. International Archives of the Photogrammetry, Remote Sensing and Spatial Information Sciences, Volume XXXVIII-1/C22, pp 25-31, September 2011, Zurich , Switzerland.